Title page

Title: Advanced body composition assessment: From body mass index to body composition profiling

Corresponding author:

Prof. Magnus Borga
Department of Biomedical Engineering
Linköping University
SE-581 83 Linköping
Sweden

Author list:

Magnus Borga[1,2,3]
Janne West[2,3,4]
Jimmy D Bell[5]
Nicholas C Harvey[6,7]
Thobias Romu[1,2,3]
Steven B Heymsfield[8]
Olof Dahlqvist Leinhard[2,3,4]

Affiliations

1. Department of Biomedical Engineering, Linköping University, Sweden
2. Center for Medical Image Science and Visualization (CMIV), Linköping University, Sweden
3. AMRA Medical AB, Linköping, Sweden
4. Department of Medical and Health Sciences, Linköping University, Sweden
5. Research Centre for Optimal Health, University of Westminster, London, UK
6. MRC Lifecourse Epidemiology Unit, University of Southampton, Southampton SO16 6YD, UK
7. NIHR Southampton Biomedical Research Centre, University of Southampton and University Hospital Southampton NHS Foundation Trust, Tremona Road, Southampton, UK
8. Pennington Biomedical Research Center, Baton Rouge, LA, US

Keywords:

Body Composition, Magnetic Resonance Imaging, UK Biobank

ABSTRACT

This paper gives a brief overview of common non-invasive techniques for body composition analysis and a more in-depth review of a body composition assessment method based on fat-referenced quantitative magnetic resonance imaging (MRI). Earlier published studies of this method are summarized, and a previously un-published validation study, based on 4.753 subjects from the UK Biobank imaging cohort, comparing the quantitative MRI method with dual-energy x-ray absorptiometry (DXA) is presented. For whole-body measurements of adipose tissue (AT) or fat and lean tissue (LT), DXA and quantitative MRI show excellent agreement with linear correlation of 0.99 and 0.97, and coefficient of variation (CV) of 4.5 % and 4.6 % for fat (computed from AT) and lean tissue respectively, but the agreement was found significantly lower for visceral adipose tissue, with a CV of more than 20 %. The additional ability of MRI to also measure muscle volumes, muscle AT infiltration and ectopic fat in combination with rapid scanning protocols and efficient image analysis tools make quantitative MRI a powerful tool for advanced body composition assessment.

INTRODUCTION

The human body – as well as the body of every other animal – is mainly composed of four molecular-level components; water, fat, proteins and minerals, usually in that order of decreasing amounts[1]. The substance that has attracted the most attention, from laypeople to medical professionals, is fat. This is, of course, motivated by the well-established fact that an excessive amount of body fat is related to increased morbidity and mortality. But also because adipose tissue (AT) is, by far, the most varying compartment – between individuals, but also within an individual over time. The most widely used way to estimate body fat is the body mass index (BMI) – body weight normalized by height squared (kg/m^2). Being a very simple and inexpensive method, it is the basis for WHO's definition of overweight ($25 \leq BMI < 30$) and obesity ($BMI \geq 30$). However, for a given BMI, the body-fat percentage changes with age, and the rate of this change is different depending on sex, ethnicity and individual differences[2]. And while BMI correlates with fat accumulation and metabolic health in large populations, it is insensitive to the actual distribution of body fat[3].

When comparing methods for body composition analysis, it is important to distinguish fat (triglyceride) from AT[4], which contains approximately 80 % fat, the rest being water, protein and minerals[5]. While most of the body fat is stored in AT, fat is also present in organs such as liver and skeletal muscle. Today, it is well known that the metabolic risk related to fat accumulation is strongly dependent on its distribution. Central obesity and, in particular, ectopic fat accumulation, are important metabolic risk factors[6-8]. Large amounts of visceral AT (VAT) are related to increased cardiac risk[8, 9], type 2 diabetes[10, 11], liver disease[12] and cancer[13, 14]. High levels of liver fat increase the risk for liver disease and type 2 diabetes[15], and increased muscle fat has been associated with increased risk for insulin resistance and type 2 diabetes[16] and reduced mobility[17]. While there are other anthropometric measures, such as waist circumference and waist-to-hip ratio, that more strongly correlate with metabolic risk[18, 19], it is now well recognized that BMI and other anthropometric surrogate measures are poor predictors for individual fat distribution and metabolic risk[3, 20, 21].

Besides fat, acting as the body's long-term energy storage, skeletal muscles are of great interest to study, and the balance between the energy-consuming muscles and the energy-storing fat compartments is, of course, highly relevant in order to understand the metabolic balance of the body. Cachexia, involuntary loss of body weight, usually with disproportionate muscle wasting, is a life-threatening condition, often related to the progression of an underlying serious disease (e.g., cancer[22]). In cancer, cachexia is defined as weight loss of more than 5% over 6 months, $BMI < 20\ kg/m^2$ or appendicular muscle mass normalized by body height squared of less than $7.26\ kg/m^2$ or $5.45\ kg/m^2$ for males and females respectively[23]. Sarcopenia, which can be related to cachexia, but is also associated with ageing, is often defined as reduced physical performance following loss of muscle mass, usually accompanied by increased fat infiltration of the muscles[24]. When diagnosing sarcopenia, muscle strength tests combined with muscle volume measurements are needed[25]. Furthermore, Willis et al. showed that muscle pathology progression over one year could be detected by quantitative MRI but not by assessing muscle strength or function[26]. These examples illustrate the need for more sophisticated body composition analysis tools that go beyond simple anthropometric measures.

Since the early part of the last century, scientists have tried to determine the body composition in different ways, with a wide range of difference physical principles and devices, and using different models and assumptions. Today, local in-vivo measurements of different fat depots and fat infiltration in organs can be made using tomographic imaging techniques such as computed tomography (CT) and magnetic resonance

imaging (MRI) that were not even invented when the first scientific studies on body composition were published. These techniques are now recognized as golden standard for body composition analysis[25, 27].

The purpose of this paper is to give a brief introduction to the most commonly used methods for body composition analysis and a review of an MRI-based body composition analysis technique, comparing its performance to other methods. This includes a previously unpublished validation study of the agreement between this method and dual-energy X-ray absorptiometry (DXA).

TECHNOLOGY OVERVIEW

A number of different techniques for body composition assessment have been developed, from very simple indirect measures such as waist-to-hip ratio and calipers to sophisticated direct volumetric measurements based on 3-dimensional imaging techniques. There are also a range of invasive or in-vitro methods for body composition analysis such as inhalation or injection of water- or fat-accumulating agents, or dissection and chemical analysis of cadavers. This overview will, however, focus solely on non-invasive in-vivo measurement techniques.

Hydrostatic Weighing (Densitometry)

Hydrostatic weighing (under-water-weighing), or densitometry, is based on Archimedes' principle. The difference of the body weight in air and in water is used to compute the body's density. Assuming a two-component model with different densities for fat mass and fat-free mass and correcting for the air volume in the lungs, the total body fat percentage can be estimated. Obviously, this technique cannot give any measurements of the distribution of AT or LT.

Air Displacement Plethysmography (ADP)

ADP is perhaps better known under its commercial brand name BOD POD (Life Measurement Inc., Concord, CA). Similar to hydrostatic weighing, ADP measures the overall body density and hence total body fat and lean tissue (LT) but not their distributions. By putting the body in an enclosed chamber and changing the chamber's volume, the volume of the displaced air (i.e., the volume of the body) can be determined from the changes in air pressure. Since ADP is based on the same two-component model as hydrostatic weighing, it is also affected by the same confounders, mainly variations in bone mineral content and hydration. Due to the limitations of the two-component model used in densitometry and ADP, a four-component (4C) model is often recommended[28, 29]. In addition to fat and LT, the 4C model also takes bone mineral content (BMC) and total body water (TBW) into account. However, these two additional components have to be measured by other techniques (e.g. dual-energy X-ray absorptiometry for the BMC, and deuterium oxide dilution for TBW[30]) The repeatability (coefficient of variation) of ADP for body fat has been reported to be between 1.7 and 4.5 % when measured within one day[31]. Obviously, ADP, as well as hydrostatic weighing, is limited to gross body composition analysis, not making any estimates of regional fat or muscles.

Bioelectrical Impedance Analysis (BIA)

BIA uses the electrical properties of the body to estimate the total body water and from that, the body fat mass[32, 33]. The body is modelled as 5 cylindrical LT compartments; the trunk and the four limbs, while fat is considered to be an insulator. The impedance is assumed to be proportional to the height and inversely proportional to the cross-sectional area of each compartment, and the electrical equivalent is a resistor (extra-cellular water) in parallel with a capacitor and a resistor in series (intra-cellular water). The model of uniform distribution of fat and water fits better to the extremities than the trunk[34], and while there are BIA measurements that correlate well with total abdominal AT, BIA cannot be used for measuring VAT[35]. Potential error sources are variations in limb length (usually estimated from body height), recent physical activity, nutrition status, tissue temperature and hydration, blood chemistry, ovulation, and electrode placement[32]. BIA requires different model parameters to be used depending on age, gender, level of physical activity, amount of body fat and ethnicity, in order to be reliable[36, 37].

Dual-energy X-ray Absorptiometry (DXA)

DXA is a two-dimensional imaging technique that uses X-rays with two different energies. The attenuation of an X-ray is dependent on the thickness of the tissue and the tissue's attenuation coefficient, which is dependent on the X-ray energy. By using two different energy levels, the images can be separated into two components (e.g., bone and soft tissue). DXA is mainly used for bone mineral density measurements, where it is considered as the gold standard[38], but it can also be used to estimate total and regional body fat and LT mass. Pixels, where the ratio between attenuations of the two energies falls below a certain threshold, are classified as soft tissue (i.e., without bone) and in those pixels, the attenuation is linearly dependent on the fat fraction of the soft tissue. Pixels above the threshold contain a mixture of bone and soft tissue, and there the soft tissue properties need to be interpolated from surrounding soft tissue pixels[39]. Approximately one third of the pixels of the projected body contains bone[40].

DXA has been found to be more accurate than density-based methods for estimating total body fat[41]. A possible confounder is that the DXA analysis assumes a constant hydration of lean soft tissue, which is not always true as hydration varies with age, gender and disease[42]. Excellent repeatability (CV) in the range 1 – 2 % for body fat and 0.5 – 2 % for LT has been reported for DXA.

Since DXA only gives a two-dimensional (coronal) projection, it is not possible to obtain direct compartmental volumetric measurements, so regional volume estimates are obtained indirectly using anatomical models. For example, VAT and parts of the subcutaneous adipose tissue (SAT), are mixed and cannot be separated in the DXA image. The distribution between VAT and SAT then needs to be estimated from an anatomical model predicting the SAT thickness. Furthermore, the physical properties of the technology do not allow for measurements of ectopic fat in organs such as liver fat or muscle fat infiltration. However, due to its ability to estimate regional fat and measure LT, in combination with relatively high availability, DXA has been used for body composition analysis in a wide range of clinical applications[43].

Computed Tomography (CT)

CT gives a three-dimensional high-resolution image volume of the complete or selected parts of the body, computed from a large number of X-ray projections of the body from different angles. The known differences in attenuations of X-rays between lean soft tissue and AT can then be used to separate these tissues, as well as to determine mixtures between them. As opposed to the previously described techniques, CT can accurately determine fat in skeletal muscle tissue[16] and in the liver[44]. It is, however, significantly less accurate for liver fat below 5 % which limits its use to diagnose low-grade steatosis[44]. Being a three-dimensional imaging technique, CT has the potential of giving direct volumetric measurements of organs and different AT depots. In practice, however, CT-based body composition analysis is in most cases limited to two-dimensional analysis of one or a limited number of axial slices of the body, leading to the utilization of the area measured as a proxy for the volume. There are two reasons for this limitation: First, it is important to keep the part of the body being scanned to a minimum in order to minimize the ionizing radiation dose[45]. This is particularly important in the ethical considerations of research studies on healthy subjects. Secondly, manual segmentation of different compartments in the images is a very labor intensive, which can be reduced by limiting the analysis to a few slices rather than a complete three-dimensional volume. This approach, however, limits its precision, since the exact locations of slices, in relation to internal organs, cannot be determined a priory, and will therefor vary between scans. Nevertheless, CT, together with MRI, are today considered the gold standards for body composition analysis, in particular regional.

Magnetic Resonance Imaging (MRI)

MRI uses the different magnetic properties of the nuclei of certain chemical elements (normally hydrogen in water and fat) in the cells to produce images of soft tissue in the body. A number of MRI-based methods for quantification of AT (see e.g. the review by Hu et al[46]) and muscles[47-52] have been developed and implemented in the past.

By using so-called "quantitative fat-water imaging", precise measurements of regional AT and LT, as well as diffuse fat infiltration in other organs, can be obtained. The basis for quantitative fat-water imaging is fat-water separated, or Dixon, imaging[53], where the different magnetic resonance frequencies of protons in fat and water are utilized for separating the two signals into a fat image and a water image. Due to a number of

undeterminable factors affecting the MR signal, an MR image is not calibrated on an absolute scale and therefore not quantitative in itself. But by using different post-processing techniques, the image can be calibrated to quantitatively measure fat or AT. Examples of such methods are proton density fat fraction (PDFF)[54] measuring the fraction of fat in MR-visible soft tissue, and fat-referenced MRI[55-57] measuring the amount of AT in each voxel.

As opposed to CT and DXA, MRI does not use ionizing radiation, which enables true volumetric three-dimensional imaging even in healthy volunteers and infants. Still, many studies using MRI for body composition analysis have used one or a limited set of two-dimensional slices, mostly due to the lack of efficient image analysis tools for handling three-dimensional image segmentation. However, since there is no ionizing radiation limiting the image acquisition, the slices can be selected from a complete image volume, thereby reducing the uncertainty in their locations. Still, using a sparse set of slices as a proxy for the complete volume will inevitably negatively affect accuracy and precision as only a fraction of the data is used. It has, for example been shown that single-slice MRI is poor at predicting VAT and SAT changes during weight loss[58, 59].

BODY COMPOSITION PROFILING USING FAT-REFERENCED MRI

Body composition profiling implies the simultaneous collection and analysis of a number of body-composition parameters, including subcutaneous and visceral AT, ectopic fat such as liver and skeletal muscle fat and muscle volumes. Fat-referenced MRI is a methodology that enables all such measurements in one single rapid examination. This section gives a brief introduction to body composition profiling using fat-referenced MRI, together with a review of published validation results of the method. Finally, a previously unpublished validation study of the agreement between this method and DXA for measurements of body fat/AT, body LT and VAT, is presented.

The body composition profiling methodology combines fat-referenced MRI with automated image segmentation of different compartments, and was first described by Dahlqvist Leinhard et al. 2008[55]. Different aspects of the method have been further described in other publications[47, 60-62]. The two key features of this method are that it produces quantitative fat-referenced images and that it uses a supervised automated segmentation tool.

In a quantitative fat-referenced image, the value in each image volume element (voxel) represents the amount of fat in that voxel in relation to the amount of fat in pure AT. Hence, a voxel in pure AT has a value of one and a voxel without any fat has the value zero. This means that the following can be measured: The total amount of AT in any given region by summation of the voxel values in that region, AT-free volume by removal of amount of AT from volume measurements of regional LT (e.g. muscles), and fractions of fat in specific internal organs, such as the liver.

The supervised automated segmentation tool enables an efficient way of segmenting different AT compartments, as well as different muscle groups, reducing the manual work to a few minutes, rather than hours, for analyzing a whole-body data set. Anatomical compartments, such as the visceral compartment and different muscle groups, are automatically segmented using predefined anatomical atlases and the operator can then adjust the segmentations if needed.

See Appendix 1 for a summary of how fat-referenced MRI is implemented in AMRA® Profiler (AMRA Medical AB, Linköping, Sweden), which is the tool for body composition profiling that was used in the validation studies of fat-referenced MRI.

Precision and Accuracy

In a previous study[61], the accuracy of body composition profiling using fat-referenced MRI, in terms of agreement with manual quantification of T1-weighted MR images, was evaluated on 23 (11 female, 12 male) subjects with an average BMI of 31.7 ± 5.1 kg/m^2 (range 22–46 kg/m^2); age 36–66 years. There was no significant difference in the measured amount of VAT (4.73 ± 1.99 versus 4.73 ± 1.75 L, p = 0.97). Furthermore, the agreement between the methods was excellent for both VAT (95 % LoA -1.06 – 1.07 L) and ASAT (-0.36 – 1.60 L). However, a very small yet statistically significant difference in ASAT was observed (10.39 ± 5.38 versus 9.78 ± 5.36 L, p < 0.001). Clearly this small difference has no clinical significance.

Test-retest repeatability and agreement with manual quantification for VAT was evaluated by Newman et al. (Newman 2016). The study included 30 subjects with five subjects from each gender for each of the following

categories of BMI: 18 – 25 kg/m^2, 25 – 30 kg/m^2 and > 30 kg/m^2. Each subject was scanned twice with at least 20 minutes interval, during which the subject left the scanner room. There was no significant difference between the evaluated method and manual quantification of VAT (p = 0.73). Bland-Altman analysis of the test-retest repeatability showed a bias of -0.04 L (95 % LoA -0.12 – 0.13 L) for VAT and 0.05 L (95 % LoA -0.55 – 0.64 L) for ASAT. The CV was 1.80 % for VAT and 2.98 % for ASAT using the method above. The CV for manual quantification of VAT was 6.33 % as a comparison.

Middleton et al. evaluated the accuracy and repeatability of VAT, ASAT and thigh muscle quantification by comparing with manual segmentation on 20 subjects[63]. Due to the laborious work with manual segmentation, 15 two-dimensional axial slices were manually segmented in the abdominal region for VAT and ASAT and 5 slices over the thigh muscles. For repeatability assessment, the subjects were scanned three times, with the subject remaining in the same position on the scan table between scan 1 and 2 and with the subject removed from the table between scan 2 and 3. The intra-examination (scan 1–2) repeatability test obtained a CV of 3.3 % for VAT, 2.2 % for ASAT and 1.5 % for total thigh muscle volume. For the inter-examination test (scan 2–3), the CVs were 3.6 %, 2. 6 % and 1.5 % for VAT, ASAT and thigh muscle volume respectively. Good agreement with the manual measurements in the 20 slices was observed for all measurements. Neither the slopes nor the intercepts of the regression lines were significantly different from those of the identity lines.

Test-retest repeatability of muscle quantification of left and right abdominal muscles, left and right, anterior and posterior thigh muscles and left and right lower limb muscles, as well as accuracy of lower leg muscle quantification were evaluated by Thomas et al[65]. comparing the method above with manual segmentation. The study included 15 subjects of each gender, ranging from normal weight to obese. Each subject was scanned twice with at least 20 minutes interval, during which the subject left the scanner room. The intra-class correlation (ICC) between the first and second scan was almost perfect (between 0.99 and 1.0) for all muscle groups. The 95 % LoA ranged from -0.04 – 0.02 L for the posterior thigh muscles to -0.15 – 0.08 L for the left lower limb. The lowest accuracy for the lower limbs was a bias of -0.08 L with 95 % LoA of -0.25 – 0.09 L.

Test-retest repeatability of measurements of VAT and ASAT volumes and volumes and fat infiltration of left and right posterior and anterior thigh muscles, lower leg muscles and abdominal muscles were evaluated by West et al. on 36 sedentary postmenopausal women[64]. Each subject was scanned twice, and the subjects were removed from the scanner room between the acquisitions. The intra-examination CV was 1.54 % for VAT, 1.06 % for ASAT, 0.8 % – 1.9 % for volumes of muscle groups (thigh, lower leg, and abdomen), and 2.3 % – 7.0 % for individual muscle volumes. The 95 % LoA was -0.13 – 0.10 L for VAT, -0.38 – 0.29 L for ASAT. The limits of agreement for liver PDFF was within ± 1.9 % and for muscle fat infiltration, it was within ± 2.06 % for muscle groups and within ± 5.13 % for individual muscles.

The method's reproducibility of fat-free muscle volume quantification between 1.5 T and 3 T MR scanners, as well as the agreement with manual segmentation, was investigated on 11 different muscle groups[47]. The ICC between the automated method and manual measurements was at least 0.97 for all muscle groups except in the arms. Except for the arms, the ICC between 1.5 T and 3 T data ranged from 0.97 (left lower leg) to 1.00 (left posterior thigh) with a mean difference volume ranging from 0.39 L (95 % LoA 0.01 – 0.77 L) (left abdomen) to 0.0 L (95 % LoA -0.10 – 0.09 L) (right lower leg). The muscles of the arms had worse accuracy and reproducibility due to difficulties to include the arms in the field of view.

Agreement with ADP

A previous study[66] compared AT measured using fat-referenced MRI with total body fat measured by ADP. The intra-class correlation was 0.984. After converting the ADP body fat measures to AT volume (assuming that most of the fat resided in AT and a density of 0.9 kg/L for AT), a Bland-Altman analysis showed that ADP underestimated AT by 0.78 L on average, but the bias was strongly dependent on the level of adiposity with significant underestimation for lean subjects and significant overestimation for subjects with higher amounts of AT. Similar bias dependence has been observed when ADP has been compared with DXA[31] and MRI[67].

Agreement with BIA

Ulbrich et al[68]. investigated the agreement between fat-referenced MRI and BIA on 80 subjects between 20 and 62 years with a BMI range from 17.5 to 26.2 kg/m^2. The linear correlation between body fat mass measured by BIA and AT volume measured by MRI was 0.75 and 0.81 for females and males respectively. The total AT measured by MRI was converted to total fat mass (again assuming that most of the fat resided in AT

and using a constant density of 0.94 kg/L). Compared to MRI, the BIA underestimated the total fat with approximately 5 kg (± 7 kg LoA) on average, this despite the fact that the MRI-based measurements of total body fat excluded the arms and lower legs. The highest linear correlation found between BIA and MRI-derived measures was 0.75 and 0.81 for females and males respectively. These correlations were found between BIA-derived body mass percentage and the MRI-derived "total AT index" (total AT divided by body height squared).

Agreement with DXA

Methods and Materials

The agreement between DXA and the fat-referenced MRI technique was assessed using data from the UK Biobank study[69], approved by the North West Multicenter Research Ethics Committee (MREC), UK, and with written informed consent obtained from all subjects prior to study entry. The age range for inclusion was 40–69 years of age. For the present analysis, participants were selected, out of the first 6,214 scanned, who had both DXA and MRI scans. One subject with obviously erroneous DXA values (2.7 kg total fat and 6.8 kg LT) was excluded, yielding a total 4,753 subjects (2,502 females and 2,251 males). All included MRI images were analyzable for VAT, ASAT and both thigh muscles according the pre-defined quality criteria[62]. The BMI range was 16.4 – 54.3 with a mean of 26.2 kg/m^2.

The MR images were acquired using a Siemens Aera 1.5 T scanner (Syngo MR D13) (Siemens, Erlangen, Germany) with the dual-echo Dixon Vibe protocol, covering neck to knees as previously described[62]. The MR images were analyzed using AMRA® Profiler. The body AT and LT were measured from the bottom of the thigh muscles to level of the top of vertebrae T9 (Figure 2). The LT was defined as the volume of soft tissue subtracted by the volume of AT[47].

Whole-body DXA data were acquired using a GE-Lunar iDXA (GE Healthcare, Madison, WI) with the subjects in supine position[70]. The images were analyzed using the GE enCORE software by the radiographer at, or soon after, the scan. The GE iDXA estimates VAT within an automatically segmented region with the lower border at the top of the iliac crest and its height is set to 20% of the distance from the top of the iliac crest to the base of the skull[71].

Since the DXA and MRI analyses measure different entities (fat and LT mass vs. AT and LT volume respectively) and they do not cover the same part of the body, a linear model was estimated by linear regression between the MRI and DXA measurements using a training data set of 2,376 randomly selected subjects. The remaining 2,377 subjects were then used for estimating the agreement between the techniques after linear transformation using the linear model (i.e., validating the linear model). The MRI-based measurements (L) were transformed to predict the DXA measurements (kg) using the linear regression coefficients from the training data, and a Bland-Altman analysis was performed to investigate the agreement between MRI- and DXA-derived measurements in the validation data. To investigate the agreement between DXA and MRI-derived VAT measurements, a linear model was estimated between the DXA and MRI measurements. Of the 4,669 subjects with available DXA VAT measurements, 2,334 cases were used to for estimate the model and the remaining 2,335 subjects were used to validate the agreement between VAT measured by MRI and the transformed DXA measurements using Bland-Altman analysis.

Results

The linear regression between MRI and DXA was 1.23 *x* - 0.12 (kg/L) for body fat/AT and 1.88 *x* + 1.82 (kg/L) for body LT. The linear correlation coefficient, r, between DXA and the transformed MRI measurements was 0.99 for body fat and 0.97 for LT. The 95 % limits of agreement from the Bland-Altman analysis were -2.25 – 2.31 kg for fat and -4.33 – 4.31 kg for LT (Figure 3). The prediction error standard deviation relative to the mean, (coefficient of variation, CV), was 4.5 % for body fat and 4.6% for LT. The correlation between VAT measured by MRI and VAT as predicted by DXA was 0.97 and the limits of agreement were -1.02 – 1.05 L, with CV = 21 % (Figure 4).

DISCUSSION

Densitometry, including ADP, shows relatively good precision, and high correlation with MRI-based measurements of whole-body AT, but with a significant volume-dependent bias. And since these methods only measure the volume or density of the body, they cannot be used for regional measurements and body composition profiling.

BIA is highly available and its relatively low cost is an advantage which also makes it useful for consumer products. Furthermore, it can differentiate intra-cellular water from extra-cellular water, which is a unique capability of BIA. BIA can also, in principle, be used for regional measurements, but it is severely limited when it comes to measuring VAT or ectopic fat in internal organs.

DXA techniques have shown good accuracy, when evaluated against MRI for whole-body measurements, and very good repeatability. The prediction of whole body fat and LT from MRI agrees well with DXA after a linear transformation, but less so for VAT. While the correlation between DXA and MRI-derived VAT was high (r = 0.97), the agreement after a linear transformation was, however, much lower than for total body fat and body LT, with a CV above 20 %. The high linear correlation, despite a modest agreement, can be explained by the very wide range of measured VAT volumes, ranging from almost zero to over 14 L. The CV for VAT is in line with the results by Kaul et al. with a CV of 15.6 % for females and 25.9 % for males when comparing the same DXA model with CT[71]. Park et al. found a linear correlation of 0.85 between VAT measured by DXA and MRI in a study including 90 non-obese men[72]. However, Kamel et al. found that the correlation was much lower (r = 0.46) for obese men[73]. The fact that the agreement is lower for obese subjects can also be observed in Figure 3 where the prediction error increases with increased VAT volume. Silver et al. found an excellent correlation without significant bias between fat-water MRI and DXA for "gross body adipose tissue" but with a significant negative bias (MRI - DXA) for "total trunk adipose tissue" as well as total and trunk LT[74]. Interestingly, for DXA, the lowest precision is for fat in the arms, with reported CV up to 11%[75]. This is the same compartment that is difficult to measure with MRI due to signal loss in the outer parts of the field of view. A strength with DXA, compared to MRI, is the simultaneous assessment of bone mineral density and mass.

When comparing different technologies, both accuracy and precision are important. Accuracy, however, can be rather difficult to compare between technologies, for several reasons. First, there is no ground truth available. Even though there is a growing consensus that tomographic methods are the gold standard that can be used to assess accuracy for other methods, they differ between themselves, and are difficult to compare in terms of accuracy. Using physical phantoms is one way to assess accuracy, but they miss the difficulties caused by anatomical variations that we know can lead to different measurement errors. Automated tomographic imaging methods can be evaluated against manual methods, but this addresses only one of several important components in the measurement system – the segmentation of different compartments. Second, not all methods measure the same thing, so even if two technologies correlate strongly, there may be a significant bias if they measure different physical entities. For example, AT is not equivalent to fat – besides fat AT also contains water, protein and minerals. When comparing a method that measures AT in volume units, such as MRI, to a method that measures fat in weight units (e.g., DXA), we have to convert one unit to the other using a density that is assumed to be constant, which again may not be always accurate.

Although this review has not focused on measurements of ectopic fat, this is an important component in body composition profiling, especially for understanding metabolic status and assessing risk. Among the techniques discussed here, CT and quantitative MRI are the only methods that can quantify local diffuse infiltration of AT and ectopic fat. (Non-invasive measurements of ectopic fat, in particular liver fat, is commonly done by MR spectroscopy (MRS), but since MRS only measures local substance concentrations and not absolute amounts of fat, AT or LT, this technology was not included in this study.) While it is possible – and sometimes necessary – to use different equipment for different measurements in a study, it is often desirable to keep the number of different examinations and modalities to a minimum in order to optimize the work flow. By using quantitative MRI, or CT if the radiation dose is not a concern, a large number of metabolically relevant body composition parameters can be measured with high accuracy and precision in a single examination.

A comparison of the capabilities of different measurements of the techniques discussed above is summarized in Table 1.

	ADP	BIA	DXA	CT	MRI
Total fat	Yes	Yes	Yes	Yes	Yes
Total lean tissue	Yes	Yes	Yes	Yes	Yes
VAT	No	No	Approximate	Yes	Yes
Volume of individual muscles	No	No	No	Yes	Yes
Diffuse fat infiltration	No	No	No	Yes	Yes
Ionizing radiation	No	No	Yes (low)	Yes	No

Table 1. Comparison of the capabilities of different techniques for body composition analysis.

CONCLUSION

There are several methods available that can measure whole-body AT or fat and LT. In terms of precision and accuracy, DXA and MRI are comparable, as they show excellent agreement after a linear transformation. However, the agreement is much lower for compartmental measurements such as VAT. Moreover, MRI gives access to accurate and direct measurements of diffuse infiltration of AT in muscles and ectopic fat (e.g., liver fat). Rapid MRI scanning protocols in combination with efficient image analysis methods have promoted MRI to a competitive option for advanced body composition assessment, thus enabling a more complete description of a person's body composition profile from a single examination.

ACKNOWLEDGEMENTS

This research has been conducted using the UK Biobank Resource under Data Access Application 6569. For full acknowledgements see Appendix 2.

COMPETING INTERESTS

Authors MB, JW, TR and ODL are employees and stock holders of AMRA Medical AB.

FINANCIAL SUPPORT

Funding support for analysis of UK Biobank data was provided by Pfizer Inc.

REFERENCES

Alphabetical order during drafting. In final manuscript numbered consecutively in the order in which they are mentioned in the text.

1. Wang ZM, Pierson Jr RN and Heymsfield SB. The five-level model: A new approach to organizing body-composition research. *American Journal of Clinical Nutrition*. 1992; 56:19-28.

2. Gallagher D, Heymsfield SB, Heo M, et al. Healthy percentage body fat ranges: an approach for developing guidelines based on body mass index. *American Journal of Clinical Nutrition*. 2000; 72:694-701.

3. Thomas EL, Frost G, Taylor-Robinson SD, et al. Excess body fat in obese and normal-weight subjects. *Nutrition Research Reviews*. 2012; 25:150-161.

4. Shen W, Wang Z, Punyanita M, et al. Adipose tissue quantification by imaging methods: a proposed classification. *Obesity Research*. 2003; 11:5-16.

5. Snyder WS. *Report of the Task group on reference man : a report.* Oxford : Pergamon, 1975; 1975.

6. Britton KA and Fox CS. Ectopic Fat Depots and Cardiovascular Disease. *Circulation*. 2011; 124:e837-e841.

7. Demerath EW, Reed D, Rogers N, et al. Visceral adiposity and its anatomical distribution as predictors of the metabolic syndrome and cardiometabolic risk factor levels. *The American Journal of Clinical Nutrition*. 2008; 88:1263-1271.

8. Liu J, Fox CS, Hickson DA, et al. Impact of Abdominal Visceral and Subcutaneous Adipose Tissue on Cardiometabolic Risk Factors: The Jackson Heart Study. *The Journal of Clinical Endocrinology and Metabolism*. 2010; 95:5419-5426.

9. Neeland IJ, Ayers CR, Rohatgi AK, et al. Associations of visceral and abdominal subcutaneous adipose tissue with markers of cardiac and metabolic risk in obese adults. *Obesity*. 2013; 21:E439-E447.

10. Iwasa M, Mifuji-Moroka R, Hara N, et al. Visceral fat volume predicts new-onset type 2 diabetes in patients with chronic hepatitis C. *Diabetes Research and Clinical Practice*. 94:468-470.

11. Kurioka S, Murakami Y, Nishiki M, et al. Relationship between Visceral Fat Accumulation and Anti-Lipolytic Action of Insulin in Patients with Type 2 Diabetes Mellitus. *Endocrine Journal*. 2002; 49:459-464.

12. van der Poorten D, Milner K-L, Hui J, et al. Visceral fat: A key mediator of steatohepatitis in metabolic liver disease. *Hepatology*. 2008; 48:449-457.

13. Britton KA, Massaro JM, Murabito JM, et al. Body Fat Distribution, Incident Cardiovascular Disease, Cancer, and All-Cause Mortality. *Journal of the American College of Cardiology*. 2013; 62:921-925.

14. Doyle SL, Donohoe CL, Lysaght J, et al. Visceral obesity, metabolic syndrome, insulin resistance and cancer. *Proceedings of the Nutrition Society*. 2011; 71:181-189.

15. Ekstedt M, Franzén LE, Mathiesen UL, et al. Long-term follow-up of patients with NAFLD and elevated liver enzymes. *Hepatology*. 2006; 44:865-873.

16. Goodpaster BH, Kelley DE, Thaete FL, et al. Skeletal muscle attenuation determined by computed tomography is associated with skeletal muscle lipid content. *Journal of Applied Physiology*. 2000; 89:104-110.

17. Marcus RL, Addison O, Dibble LE, et al. Intramuscular Adipose Tissue, Sarcopenia, and Mobility Function in Older Individuals. *Journal of Aging Research*. 2012; 2012:629637.

18. Chan DC, Watts GF, Barrett PHR, et al. Waist circumference, waist-to-hip ratio and body mass index as predictors of adipose tissue compartments in men. *QJM: An International Journal of Medicine*. 2003; 96:441-447.

19. Hsu C-H, Lin J-D, Hsieh C-H, et al. Adiposity measurements in association with metabolic syndrome in older men have different clinical implications. *Nutrition Research*. 2014; 34:219-225.

20. Prentice AM and Jebb SA. Beyond body mass index. *Obesity Reviews*. 2001; 2:141-147.

21. Tomiyama AJ, Hunger JM, Nguyen-Cuu J, et al. Misclassification of cardiometabolic health when using body mass index categories in NHANES 2005–2012. *International Journal of Obesity*. 2016; 40:883-886.

22. Morley JE, Thomas DR and Wilson M-MG. Cachexia: pathophysiology and clinical relevance. *The American Journal of Clinical Nutrition*. 2006; 83:735-743.

23. Fearon K, Strasser F, Anker SD, et al. Review: Definition and classification of cancer cachexia: an international consensus. *Lancet Oncology*. 2011; 12:489-495.

24. Cruz-Jentoft AJ and Morley JE. *Sarcopenia. .* Chichester, West Sussex ; Hoboken, N.J. : Wiley-Blackwell, 2012.; 2012.

25. Cruz-Jentoft AJ, Baeyens JP, Bauer JM, et al. Sarcopenia: European consensus on definition and diagnosis: Report of the European Working Group on Sarcopenia in Older People. United States, North America: Oxford University Press; 2010.

26. Willis TA, Eagle M, Mayhew A, et al. Quantitative Muscle MRI as an Assessment Tool for Monitoring Disease Progression in LGMD2I: A Multicentre Longitudinal Study. *PLoS ONE*. 2013; 8.

27. Thomas EL, Fitzpatrick JA, Malik SJ, et al. Whole body fat: Content and distribution. *Progress in Nuclear Magnetic Resonance Spectroscopy*. 2013; 73:56-80.

28. Baumgartner RN, Heymsfield SB, Lichtman S, et al. Body composition in elderly people: effect of criterion estimates on predictive equations. *The American Journal of Clinical Nutrition*. 1991; 53:1345-1353.

29. Bergsma–Kadijk JA, Baumeister B and Deurenberg P. Measurement of body fat in young and elderly women: comparison between a four-compartment model and widely used reference methods. *British Journal of Nutrition*. 1996; 75:649-657.

30. Forbes GB. *Human body composition : growth, aging, nutrition, and activity.* Springer-Verlag; 1987.

31. Fields DA, Goran MI and McCrory MA. Body-composition assessment via air-displacement plethysmography in adults and children: a review. *The American Journal of Clinical Nutrition*. 2002; 75:453-467.

32. Stahn A, Terblanche E and Gunga H-C. Use of Bioelectrical Impedance: General Principles and Overview. In: V. R. Preedy, ed. *Handbook of Anthropometry: Physical Measures of Human Form in Health and Disease*. New York, NY: Springer New York; 2012:49-90.

33. Khalil SF, Mohktar MS and Ibrahim F. The Theory and Fundamentals of Bioimpedance Analysis in Clinical Status Monitoring and Diagnosis of Diseases. *Sensors (Basel, Switzerland)*. 2014; 14:10895-10928.

34. Kyle UG, Bosaeus I, De Lorenzo AD, et al. ESPEN GUIDELINES: Bioelectrical impedance analysis—part I: review of principles and methods. *Clinical Nutrition*. 2004; 23:1226-1243.

35. Browning LM, Mugridge O, Chatfield M, et al. Validity of a new abdominal bioelectrical impedance device to measure abdominal and visceral fat: comparison with MRI. *Obesity (Silver Spring, Md)*. 2010; 18:2385-2391.

36. Dehghan M and Merchant AT. Is bioelectrical impedance accurate for use in large epidemiological studies? *Nutrition Journal*. 2008; 7:26-26.

37. Haroun D, Taylor SJC, Viner RM, et al. Validation of Bioelectrical Impedance Analysis in Adolescents Across Different Ethnic Groups. *Obesity*. 2010; 18:1252-1259.

38. Garg MK and Kharb S. Dual energy X-ray absorptiometry: Pitfalls in measurement and interpretation of bone mineral density. *Indian Journal of Endocrinology and Metabolism*. 2013; 17:203-210.

39. Webber CE. Reproducibility of DXA Measurements of Bone Mineral and Body Composition: Application to Routine Clinical Measurements. In: V. R. Preedy, ed. *Handbook of Anthropometry: Physical Measures of Human Form in Health and Disease*. New York, NY: Springer New York; 2012:151-165.

40. Laskey MA. Dual-energy X-ray absorptiometry and body composition. *Nutrition*. 1996; 12:45-51.

41. Prior BM, Cureton KJ, Modlesky CM, et al. In vivo validation of whole body composition estimates from dual-energy X-ray absorptiometry. *Journal of Applied Physiology*. 1997; 83:623.

42. Siri WE. The gross composition of the body. *Advances In Biological And Medical Physics*. 1956; 4:239-280.

43. Albanese CV, Diessel E and Genant HK. Review Article: Clinical Applications of Body Composition Measurements Using DXA. *Journal of Clinical Densitometry*. 2003; 6:75-85.

44. Kramer H, Pickhardt PJ, Kliewer MA, et al. Accuracy of Liver Fat Quantification With Advanced CT, MRI, and Ultrasound Techniques: Prospective Comparison With MR Spectroscopy. *AJR American journal of roentgenology*. 2017; 208:92-100.

45. Yu L, Liu X, Leng S, et al. Radiation dose reduction in computed tomography: techniques and future perspective. *Imaging in medicine*. 2009; 1:65-84.

46. Hu H, Chen J and Shen W. Segmentation and quantification of adipose tissue by magnetic resonance imaging. *MAGMA: Magnetic Resonance Materials in Physics, Biology & Medicine*. 2016; 29:259.

47. Karlsson A, Romu T, Borga M, et al. Automatic and quantitative assessment of regional muscle volume by multi-atlas segmentation using whole-body water-fat MRI. *Journal of Magnetic Resonance Imaging*. 2015; 41:1558-1569.

48. Andrews S and Hamarneh G. The Generalized Log-Ratio Transformation: Learning Shape and Adjacency Priors for Simultaneous Thigh Muscle Segmentation. *IEEE Transactions on Medical Imaging*. 2015; 34:1773-1787.

49. Lareau-Trudel E, Le Troter A, Ghattas B, et al. Muscle Quantitative MR Imaging and Clustering Analysis in Patients with Facioscapulohumeral Muscular Dystrophy Type 1. *PLoS ONE*. 2015; 10:1-16.

50. Orgiu S, Lafortuna CL, Rastelli F, et al. Automatic muscle and fat segmentation in the thigh from T1-Weighted MRI. *Journal of Magnetic Resonance Imaging*. 2016; 43:601-610.

51. Ugarte V, Sinha U, Malis V, et al. 3D multimodal spatial fuzzy segmentation of intramuscular connective and adipose tissue from ultrashort TE MR images of calf muscle. *Magnetic Resonance in Medicine*. 2017; 77:870-883.

52. Yang YX, Chong MS, Tay L, et al. Automated assessment of thigh composition using machine learning for Dixon magnetic resonance images. *Magma (New York, NY)*. 2016; 29:723-731.

53. Dixon W. Simple proton spectroscopic imaging. *Radiology*. 1984:189-194.

54. Reeder SB, Hu HH and Sirlin CB. Proton density fat-fraction: A standardized mr-based biomarker of tissue fat concentration. *Journal of Magnetic Resonance Imaging*. 2012; 36:1011-1014.

55. Dahlqvist Leinhard O, Johansson A, Rydell J, et al. Quantitative Abdominal Fat Estimation Using MRI. *INTERNATIONAL CONFERENCE ON PATTERN RECOGNITION*. 2008; CONF 19:2137-2140.

56. Hu HH and Nayak KS. Quantification of Absolute Fat Mass Using an Adipose Tissue Reference Signal Model. *Journal of magnetic resonance imaging : JMRI*. 2008; 28:1483-1491.

57. Romu T, Borga M and Dahlqvist Leinhard O. MANA - Multi scale adaptive normalized averaging. *2011 IEEE International Symposium on Biomedical Imaging: From Nano to Macro*. IEEE conference proceedings; 2011:361-364.

58. Thomas EL and Bell JD. Influence of undersampling on magnetic resonance imaging measurements of intra-abdominal adipose tissue. *International Journal Of Obesity*. 2003; 27:211.

59. Shen W, Chen J, Gantz M, et al. A Single mri Slice Does Not Accurately Predict Visceral and Subcutaneous Adipose Tissue Changes During Weight Loss. *Obesity*. 2012; 20:2458-2463.

60. Romu T, Dahlqvist Leinhard O, Forsgren M, et al. Fat Water Classification of Symmetrically Sampled Two-Point Dixon Images Using Biased Partial Volume Effects. *Proceedings of the annual meeting of the International Society for Magnetic Resonance in Medicine (ISMRM 2011), 2011 :*. 2011.

61. Borga M, Romu T, Rosander J, et al. Validation of a fast method for quantification of intra-abdominal and subcutaneous adipose tissue for large-scale human studies. *NMR in Biomedicine*. 2015; 28:1747-1753.

62. West J, Dahlqvist Leinhard O, Romu T, et al. Feasibility of MR-Based Body Composition Analysis in Large Scale Population Studies. *PLOS ONE*. 2016; 11:e0163332.

63. Middleton MS, Haufe W, Hooker J, et al. Quantifying abdominal adipose tissue and thigh muscle volume and hepatic proton density fat fraction: Repeatability and accuracy of an MR imaging-based, semiautomated analysis method. *Radiology*. 2017; 283:438-449.

64. West J, Romu T, Thorell S, et al. Precision of MRI-based body composition measurements of postmenopausal women. *PLOS ONE*. 2018; 13:e0192495.

65. Thomas MS, Newman D, Leinhard OD, et al. Test-retest reliability of automated whole body and compartmental muscle volume measurements on a wide bore 3T MR system. *European Radiology*. 2014.

66. Thunón P, Romu T, Zanjanis S, et al. Body Composition Volumetry by Whole-Body Water-Fat Separated MRI. *ISMRM 22nd Annual Meeting & Exhibition, 10 - 16 May 2014, Milan, Italy*. 2014.

67. Ludwig UA, Klausmann F, Baumann S, et al. Whole-body MRI-based fat quantification: A comparison to air displacement plethysmography. *Journal of Magnetic Resonance Imaging*. 2014.

68. Ulbrich EJ, Nanz D, Leinhard OD, et al. Whole-body adipose tissue and lean muscle volumes and their distribution across gender and age: MR-derived normative values in a normal-weight Swiss population. *Magnetic Resonance in Medicine*. 2017.

69. Sudlow C, Gallacher J, Allen N, et al. UK Biobank: An Open Access Resource for Identifying the Causes of a Wide Range of Complex Diseases of Middle and Old Age. *PLOS Medicine*. 2015; 12:e1001779.

70. Harvey NC, Matthews P, Collins R, et al. Osteoporosis epidemiology in UK Biobank: a unique opportunity for international researchers. *Osteoporosis international : a journal established as result of cooperation between the European Foundation for Osteoporosis and the National Osteoporosis Foundation of the USA*. 2013; 24:2903-2905.

71. Kaul S, Shapiro MD, Rothney MP, et al. Dual-energy X-ray absorptiometry for quantification of visceral fat. *Obesity*. 2012; 20:1313-1318.

72. Park YW, Heymsfield SB and Gallagher D. Are dual-energy X-ray absorptiometry regional estimates associated with visceral adipose tissue mass? *International Journal of Obesity & Related Metabolic Disorders*. 2002; 26:978.

73. Kamel EG, McNeill G and Van Wijk MCW. Usefulness of anthropometry and DXA in predicting intra-abdominal fat in obese men and women. *Obesity Research*. 2000; 8:36-42.

74. Silver HJ, Niswender KD, Kullberg J, et al. Comparison of Gross Body Fat-Water Magnetic Resonance Imaging at 3 Tesla to Dual-Energy X-Ray Absorptiometry in Obese Women. *Obesity*. 2013; 21:765-774.

75. Cordero-MacIntyre ZR, Peters W, Libanati CR, et al. Original Article: Reproducibility of DXA in Obese Women. *Journal of Clinical Densitometry*. 2002; 5:35-44.

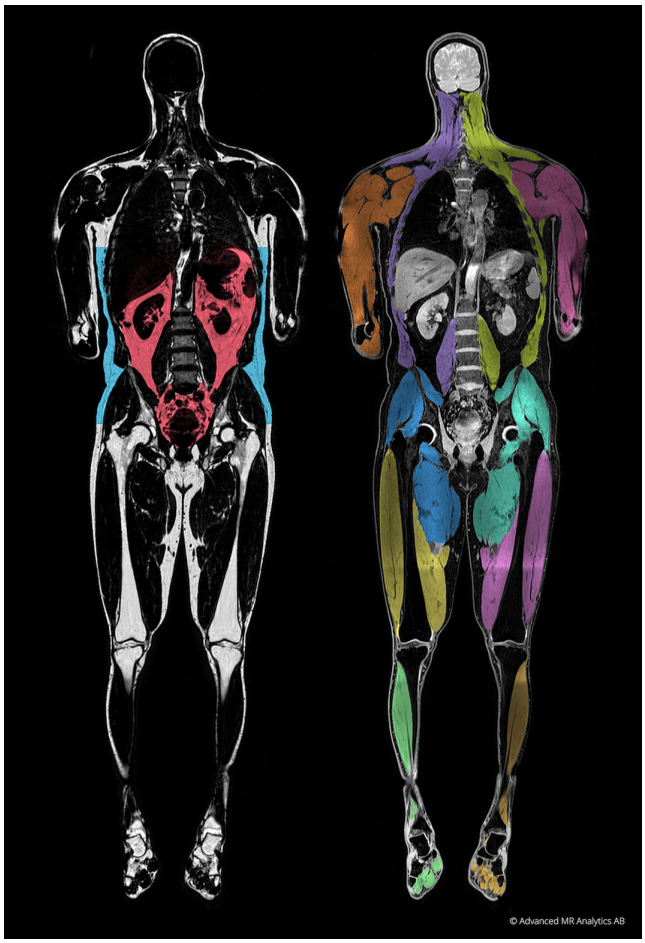

Figure 1. Example of segmentation of abdominal subcutaneous AT (ASAT), visceral AT (VAT) and 10 muscle groups from fat-water separated MRI using fat-referenced MRI and multi-atlas image segmentation. To the left is the fat image with ASAT (blue) and VAT (red), and to the right is the water image with the different muscle groups colored. (Reproduced with permission from AMRA Medical AB.)

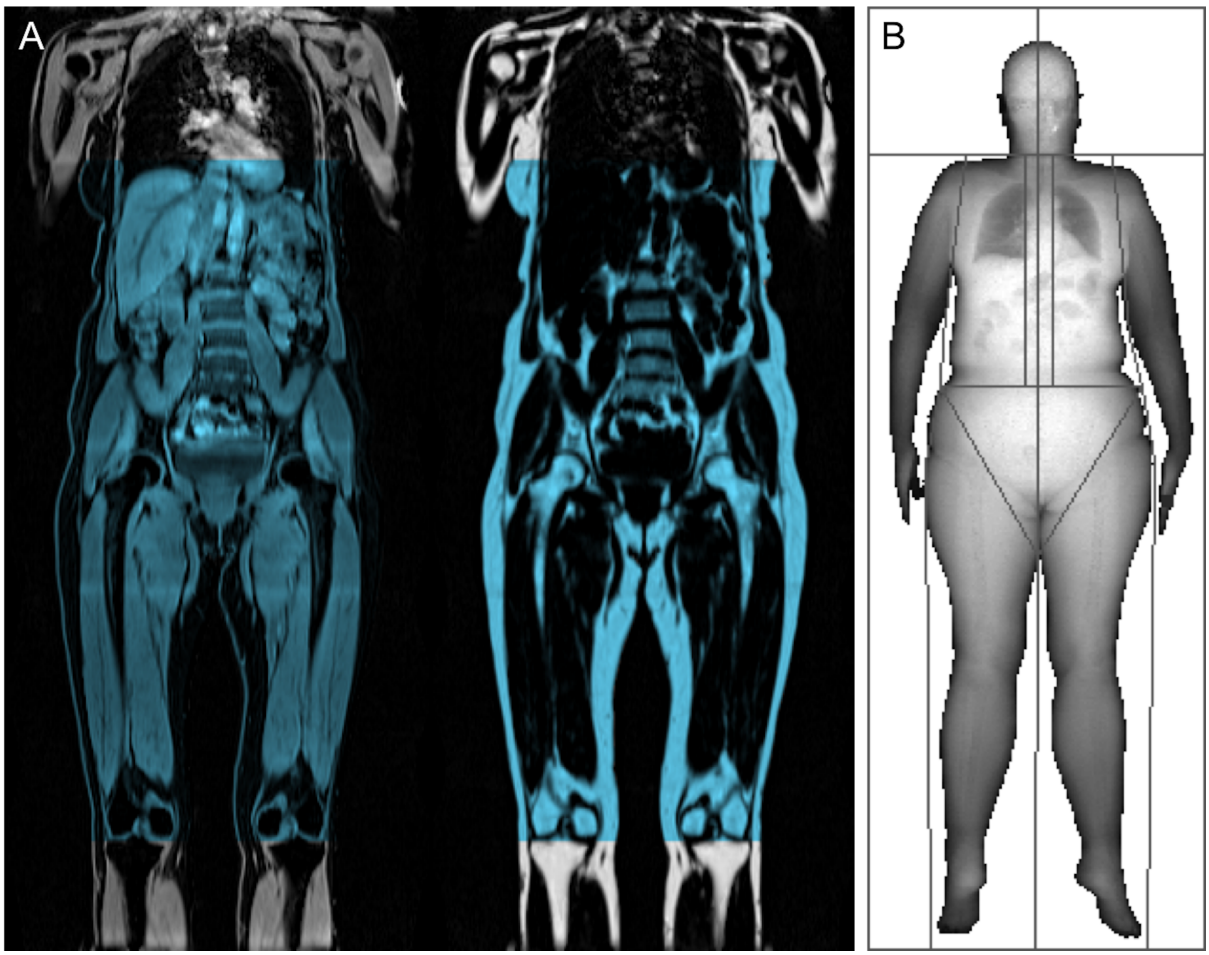

Figure 2. A: The definition of lean and adipose tissue measured by MRI from the bottom of the thigh muscles to top of vertebrae T9 marked in blue color in the water (left) and fat (right) image. B: An example of a DXA image from the study cohort. (DXA image copyright UK Biobank. Reprinted with permission.)

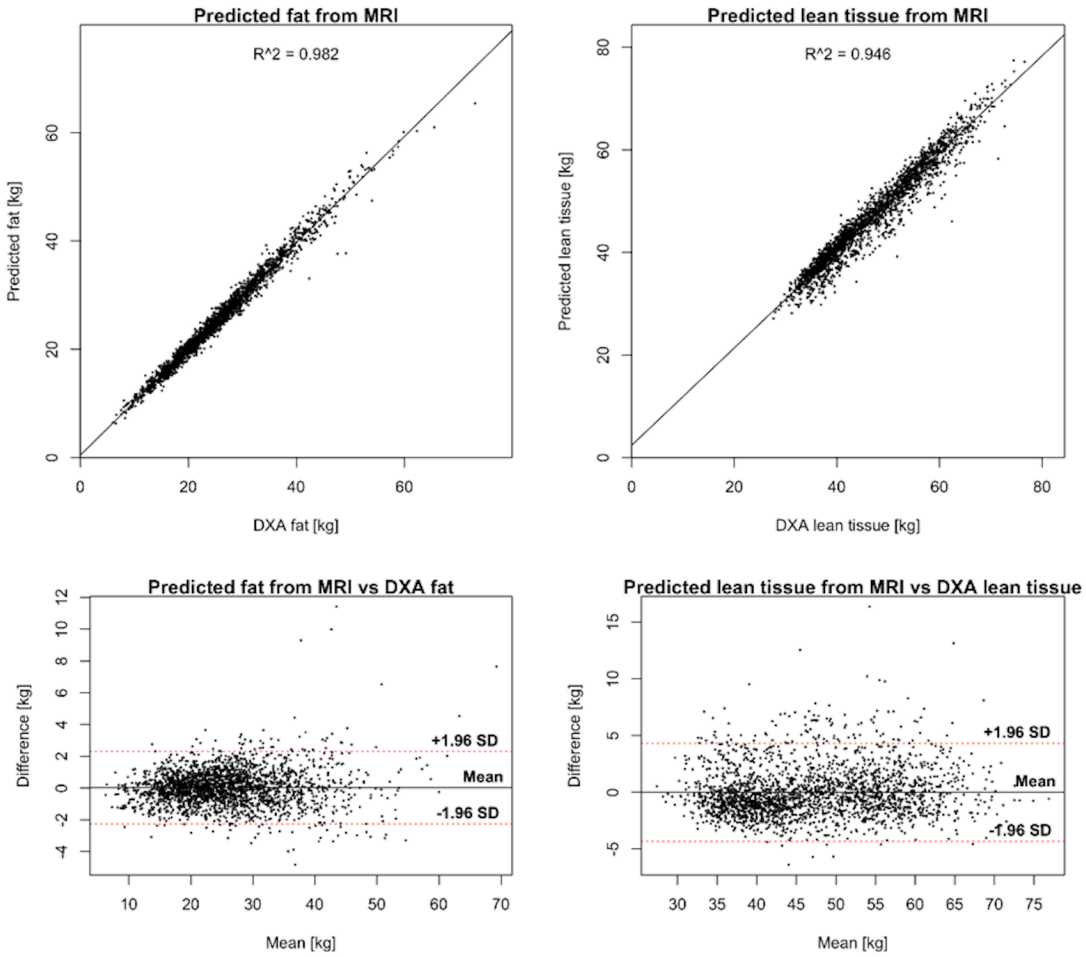

Figure 3. Correlation plots (upper row) between DXA and corresponding measurement predicted from MRI using a linear transformation for body fat (left) and body LT (right). The bottom row shows Bland-Altman plots of the agreement between DXA and corresponding measures predicted from MRI.

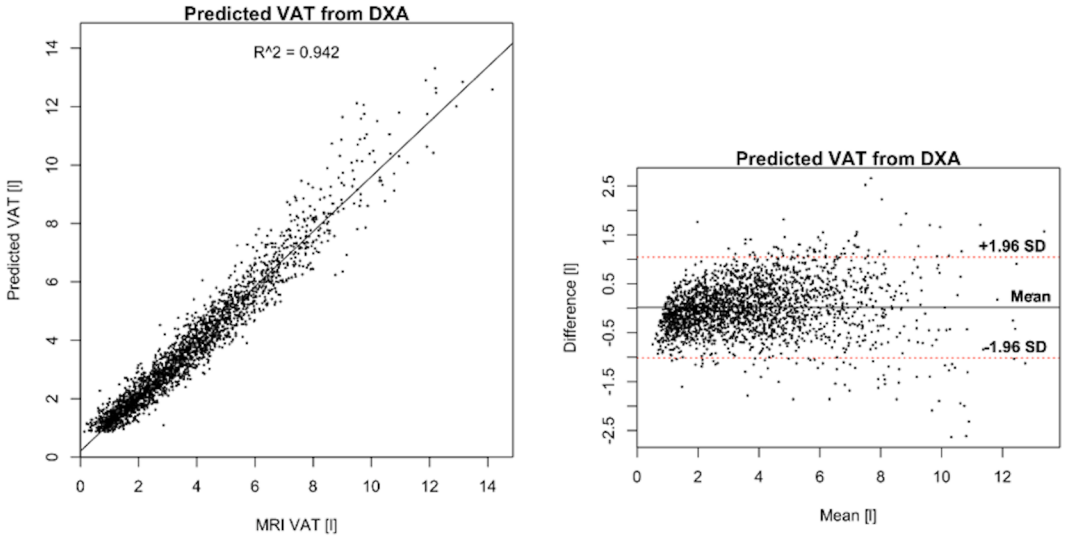

Figure 4. Correlation between VAT predicted by DXA and VAT measured by MRI (left) and Bland-Altman plot showing the agreement (liters) between the methods (right).